A 2D nano-positioning system with a sub-nanometric repeatability over millimetre displacement range

Luc Chassagne, Marwan Wakim, Suan Xu, Suat Topsu, Pascal Ruaux, Patrick Juncar, Yasser Alayli

2D nano-positioning system with a sub-nanometric repeatability over millimetre displacement range

L Chassagne[1], M Wakim[1], S Xu[1], S Topçu[1], P Ruaux[1], P Juncar[2] and Y Alayli[1]

[1] LISV, University of Versailles Saint-Quentin, 45 avenue des Etats Unis F78035 Versailles, France
[2] INM/CNAM, 292 rue Saint Martin 75141 Paris cedex, France

luc.chassagne@ens-phys.uvsq.fr

Abstract

We propose a 2D displacement control system with a sub-nanometric repeatability on position over millimetre travel range on both axes. It could be useful for nanofabrication processes or other applications related to the nanotechnology community. In our case, the apparatus is planned to be used in atomic force microscopes and lithography systems as sample-holding device. The method is based on a heterodyne interferometric sensor and a home-made high frequency phase-shifting electronic board. This paper presents the complete mechanical system and gives experimental results showing repeatability of 0.5 nm over a dynamic range of 5 mm.

1. Introduction

A major obstacle nanotechnology faces today is the lack of effective devices for building and characterizing nanoscale structures. In many fields of nanotechnology and even in the field of nanomanipulation, the accuracy and the repeatability on the displacement of the sample-holders are critical parameters whatever the approach is top-down or bottom-up [1]. Controlling the position of a mechanical system with a sub-nanometric accuracy over a dynamic range of several millimeters is one of the key factors for the development of these domains. Although state of the art apparatus can perform displacements over millimeter range with resolution at the nanometric scale, their repeatability and accuracy are still above tens of hundreds of nanometers mainly limited by the mechanical defects of the translation stage. In Ref. [2-3], authors have developed mechanical systems with a high resolution step displacement and a well-controlled flatness and straightness. However, their accuracy in positioning reaches at best 100 nm [4]. The technological progress, notably in the field of photolithography, leaves us to think that this point will be a serious technological bolt in the near future [5]. In near field microscopy, apparatus like Scanning Probe Microscopes (SPMs) can perform scans over 100 μm limited by the dynamic range of the piezoelectric actuators. Numerous works are performed to extend this scanning range [6-8]. Most of them consist of coupling transducers to a mechanical amplifier increasing hence the travel range but reducing the bandwidth of the system. Even in theses cases, the displacement ranges are limited to less than a millimeter. Another solution consists on coupling a long range displacement stage to an accurate short range one so as to compensate its defects [9-11]. In Ref. [11], authors use a two-dimensional flexure stage combined with a piezoelectric actuator. A digital closed-loop composed by a laser interferometer allows them to reach accuracy of 1 nm but for a displacement less than 0.1 mm. In Ref. [12], the moving stage is based on a magnetically suspended precision motion control stage with six degrees of freedom. The travel range is 25 mm × 25 mm. The positioning noise level is 0.6 nm (3σ). They expect to reach an accuracy of 10 nm.

Another key parameter is the traceability of the dimensional measurements made at this scale. SPMs are used

frequently to measure surface features and parameters. The calibration of the image scales is a prerequisite condition for establishing a quality process. Metrological atomic force microscopes (MAFM) are under development in several laboratories [13-15]. Most of them are planned to be used only over tens micrometers due to the difficulties making long range accurate displacements.

We propose a long range displacement nanopositioning device which combines at time, traceability, sub-nanometric repeatability and millimeter range displacement. This system is based on a specific phase-shifting high frequency electronic board, a heterodyne interferometer and a dual XY translation stage. The results presented in this paper show that our system can fulfill metrological requirements for applications in nanometrology, nanomanipulation or nanoassembly. The aim of the project is to control the sample-holder integrated in a near field probe microscope in order to scan large scale images with nanometric accuracy. We also plan to use the system for long range electronic beam lithography processes.

2. Design overview

2.1. Principle of the servo-loop of the system

We developed an optoelectronic system board which controls the position of a moving mirror with sub-nanometric accuracy [16] (figure 1). The heterodyne interferometer has a heterodyne frequency of 20 MHz [17]. The information on the position of the moving mirror is deduced by comparing the phases of the optical beams incoming and outcoming from the interferometer. A high frequency electronic board performs two signals at the heterodyne frequency of 20 MHz. One of these signals S_1 is sent onto the laser head to perform the two synchronous signals at the heterodyne frequency. The second one S_2 is used as a reference and is phase compared with the phase of the signal S_3 coming from the output of the interferometer. Some phase shifts can be done either on the S_1 signal or on the S_2 signal thanks to a computer. The phase of the signal S_3 at the output of the heterodyne interferometer is locked-in on the phase of the signal S_2 via an analog servo-loop.

If a phase shift is made on the signal S_2, the servo-loop moves the mirror to compensate this phase shift using the Doppler effect. If the phase shift is made on the signal S_1, the mirror moves in the other way. The hysteresis, the creep and non-linearity phenomena of the piezoelectric actuator are non-relevant because the lock-in servo loop takes the information from the phase of the interferometer [18].

Hence it is possible to control the position of the target mirror by controlling the phase shift applied on the signals S_1 or S_2.
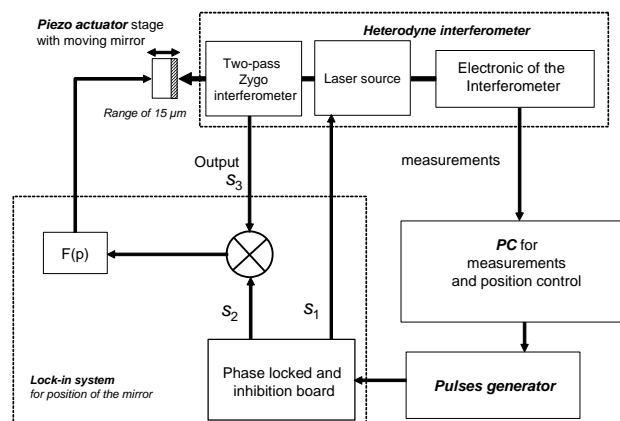

Figure 1: Principle of the Servo-loop control. The position of the target mirror is controlled via the phase of the heterodyne signal issue from the interferometer using an analog servo-loop.

The phase locked electronic board is composed of an ultra-high stability oscillator at a frequency of 10 MHz. A Phase Locked Loop (PLL) generates the two signals at the frequency of 20 MHz. A Phase Shifting Electronic (PSE) circuit can impose some phase shift of $\Delta\phi = 2\pi / p$ on these signals. The factor p is digitally programmable with the PC link. For a two-pass interferometer, a phase change of 2π corresponds to a moving of $\lambda_0/4n$ where λ_0 is the

wavelength under vacuum of the laser source and n the refractive index of the air. The displacement corresponding to a phase shift of $\Delta\phi$ is

$$\Delta d = \frac{\lambda_0 \Delta\phi}{8\pi n} \qquad (1)$$

We use a frequency stabilized red line Helium-Neon laser which has been calibrated in regard to a national reference at the Laboratoire National de métrologie et d'Essais (LNE, France). Its wavelength under vacuum is equal to $\lambda_0 = 632.991528$ nm with a relative uncertainty of $1.6 \ 10^{-9}$ (1σ). Phase shifts are controlled with command pulses via a digital pulse generator. As the phase shift is generated numerically, the uncertainty on the position steps is mainly limited by the uncertainty on the laser wavelength. Experimental results have been demonstrated with position step as small as 0.25 nm and repeatability below one nanometre for micrometric range displacements. More details can be found in Ref. [18].

2.2. Setup of the 2D extended system

We extended the method for a long range and two-dimension displacements. For this purpose, we developed two axes XY moving system associated with a dual servo-control (figure 2). A first stage is composed of two linear motors $ST1_X$ and $ST1_Y$ (Aerotech ANT50) which can move over 50 mm with their own lock-in system based on Proportional Integral Derivative unit (PID). Their resolutions are 10 nm, limited by the encoder used in the servo loop. The flatness and the straightness are below 1μm. The second level stage is two axes piezoelectric actuators PZT_{XY} (PiezoSystem, Jena) with a displacement range of 15 μm and a sub-nanometric resolution. It has been chosen for its high cut-off frequency (2.5 kHz in both axes). The target mirrors are two orthogonal faces of a Zerodur® cube with a 20 mm edge. The defect of orthogonality between both faces is less than 1 sec. This cube is adjusted in regard to the piezoelectric actuators using a rotating element. The whole system is assembled onto the ST1 unit as illustrated in figure 3. The orthogonality between the two translation axes of the motors has been controlled by an interferometric technique with an accuracy of 5 arcsec.
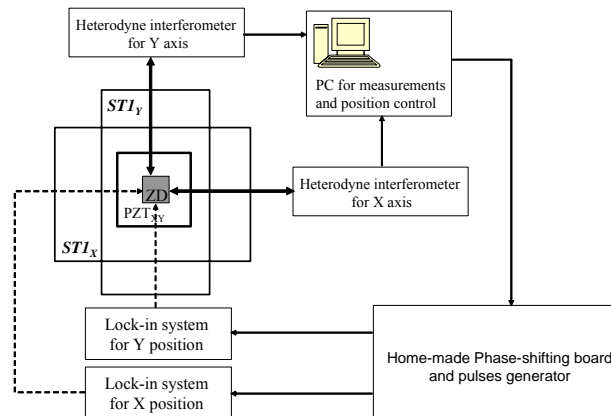

Figure 2: Principle of the two dimensions long range displacements system. ZD-Zerodur Cube; $ST1_{X,Y}$ – long range displacement linear motors; $PZT_{X,Y}$ - piezoelectric actuator.

The two heterodyne interferometers measure the position of the mirrors with a resolution of 0.31 nm. A weather station is used to calculate the refractive index of air using the Edlén formula [19]. The displacements are programmable with a Labview software interface and a data acquisition card. The current position is monitored and a numeric field can be filled to compute the trajectory. The home-made PSE electronic board generates the phase-shifts which are necessary to control the phase lock-in system described above and associated with the PID unit.
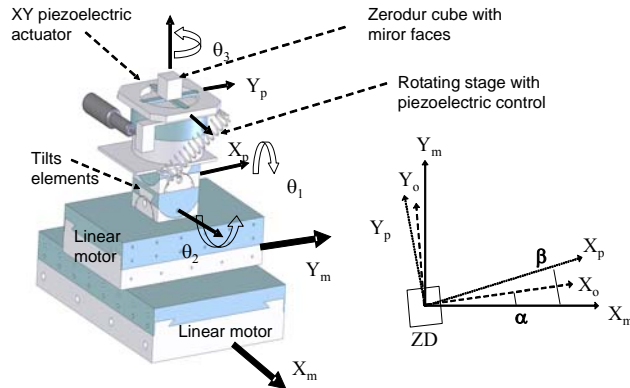
Figure 3: 3D overview of the system. $(X_m; Y_m)$ are the displacement axes of the long range stages; $(X_p; Y_p)$ are the axes of the piezoelectric actuators; $(X_o; Y_o)$ are the axes of the mirror cube. The angles α and   are respectively the misalignment angles between $(X_m; Y_m)$-$(X_o; Y_o)$ and between $(X_m; Y_m)$ -$(X_p; Y_p)$.

The resolution steps are programmable independently for both axes. In figure 4, we report a displacement in an XY plane with 10 nm steps in the Y direction and 5.6 nm steps in the X direction. The frequency of the steps is 1 Hz and the sample frequency of the sensor is 150 Hz. Due to the optical nonlinearities of the heterodyne interferometer, a low periodic discrepancy is observed. This error has been estimated to 2 nm. However it could be less than 1 nm as described in Ref. [20-23].
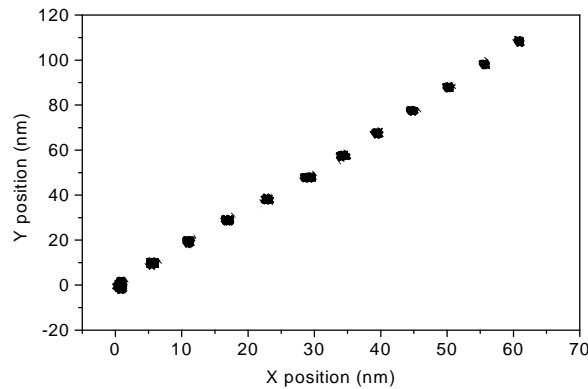

Figure 4: Displacement in an XY plane with 10 nm steps in the Y direction and 5.6 nm steps in the X direction. The low periodic discrepancy is due to the optical nonlinearities of the heterodyne interferometer.

2.3. System operation

The position control system can process with two different configurations. In the first one, we named "free mode", the stages ST1 and ST2 are independent. Long range displacements are performed with ST1 while ST2 stage is disabled. Near the target point, ST2 is enabled and steps are generated with PSE to reach accurately the target position using the method described above. Hence it compensates the defects of the first stage only on the target position. The displacement range of the entire system is limited by the straightness ST1 which must be less than the displacement range of the piezoelectric actuator. In our case, using a piezoelectric actuator with a 3 μm travel range, the movable mirror has been displaced over 5 mm without breaking the loop. In the second configuration, named "trajectory mode", both actuators are enabled simultaneously. Phase-shifts are generated by the PSE all over the displacement path in order to compensate the defects of ST1 until the target point. Previous works in this configuration have been demonstrated to control accurately the velocity of a one kilogram mass [24]. These two

configurations are complementary. The "free mode" configuration is less accurate than the "trajectory mode" but it is suited for applications which require rapidity and where the path is not relevant. The "trajectory mode" is more accurate but slower. It is appropriate for applications which require position control all over the path.

3. Experimental setup

3.1. Nanopositioning performances

In order to illustrate the possibilities of our system the software calculates specific commands to draw trajectories as reported in figure 5. This set of trajectories has been realized in the "free mode" configuration. The starting point is located at X=0 and Y = 250 nm. Firstly, the system operates a circular path of 250 nm of radius, then a square motion of a same size, and finally a diamond. The X and Y positions are controlled with position steps with a resolution equal to 4.9 nm for both axes. In this example, each trajectory takes about one minute to complete.
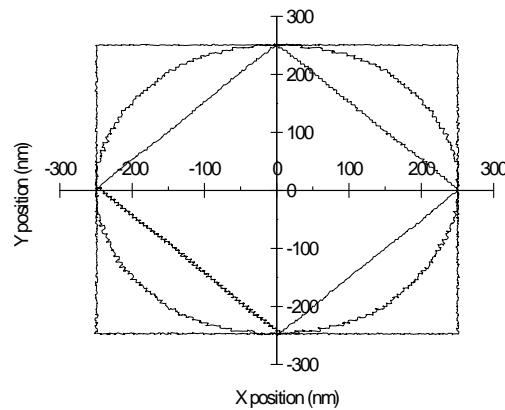

Figure 5: Example of trajectories made with our nanodisplacement system. The starting point is located at X=0 and Y = 250 nm. Firstly, the system operates a circular path of 250 nm of radius, then a square motion of a same size, and finally a diamond.

The data acquisition rate is 1.5 kHz without any averaging. To measure the repeatability, 25 consecutive sequences of square trajectories have been launched. The standard deviations of the position around the top right corner of the square are 3.0 nm for the X axis and 2.2 nm for the Y axis.

The repeatability has been also measured over long range motions. For this purpose, the system is programmed in the "free mode" configuration to make back and forth displacements from a point A to a point B far from 5 mm along the X axis. The velocity is 1 mm.s^{-1}. The resolution of the step position made with ST2 is 0.25 nm. The experiment is repeated 20 times. The repeatability is defined as the standard deviation of the positioning error x_A-x'_A where x_A is the starting position and x'_A is the position after the back and forth displacement. The result is depicted in figure 6.
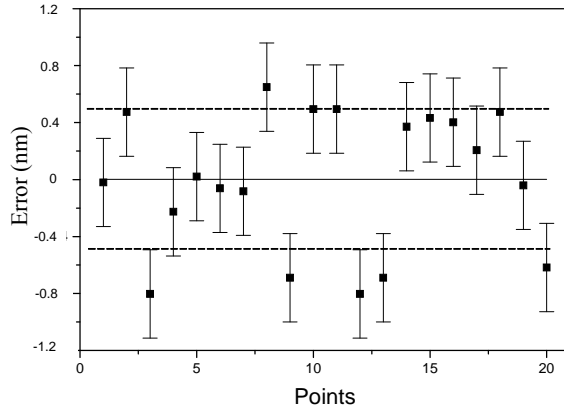
Figure 6: Repeatability for long range displacements. A sequence of 20 back and forth displacements of 5 mm is launched. The straight line represents the mean value and the doted lines the standard deviation which is equal to 0.5 nm.

3.2. Compensation of defects along the path

The "trajectory mode" configuration is more appropriate for long range motions due to the control of the position at every point of the trajectory. However for long range displacement, the alignments between all axes are critical. In this section, we point out the error in positioning due to the two main sources of misalignment. The first is the misalignment between the optical path and the mechanical one. The second misalignment is the orthogonality defect between the X and Y axes.

As defined in figure 3, the mechanical axes are noted respectively $(X_m; Y_m)$ for the long range mechanical stages, and $(X_p; Y_p)$ for the piezoelectric actuator. The main axes of the mirror cube are noted $(X_o; Y_o)$. The angle α is the misalignment angle between $(X_m; Y_m)$ and $(X_o; Y_o)$ and   the angle between $(X_m; Y_m)$ and $(X_p; Y_p)$. Ideally, α and β are null. In the real case, small values of α or β exist. This will induce a first source of a cosine error on the displacement given by $\varepsilon = L \times \theta^2 / 2$ where   is equal to α or β and L the displacement [25]. This error remains negligible for millimetre range displacements and for misalignments less than 1 mrad, which is easily done with classical optical alignment techniques.

The second source of error occurs when a displacement is made on X_m or X_p axis and the Y_o axis is not perfectly orthogonal. This leads to a tangential error on Y axis given by $\varepsilon_Y = L_X \times \theta$ where L_X is the displacement along the X axis. A similar error ($_X$) occurs when the displacement is along Y_m or Y_p axis. Let   = 17 mrad and $L_X = 3$ μm, ε_Y is less than 50 nm. Due to the short range displacement of the PZT actuator, the alignment between the $(X_p; Y_p)$ and the $(X_o; Y_o)$ axes is far less critical and could be done by conventional mechanical adjustments.

For a longer motion $L_X = 5$ mm, ε_Y is equal to 85 μm. Hence, the alignment between the $(X_m; Y_m)$ and the $(X_o; Y_o)$ axes becomes very critical and requires a specific procedure. We developed a very fine voltage-controlled rotating stage composed of a mechanical rotating element and a piezoelectric actuator. The resolution of the rotating stage is below 100 nrad which leads to a resolution on ε_Y below to 0.5 nm for $L_X = 5$ mm. The capability of this system is illustrated in figure 7. Displacements of 5 mm are performed along X_m. The velocity of the motion is 1 mm.s^{-1}. Simultaneously the optical path variation is measured along Y_0 leading to displacements reported in figure 7(a). This process is repeated until the ε_Y is below to 1 nm by tuning the rotating stage (figure 7(b)).
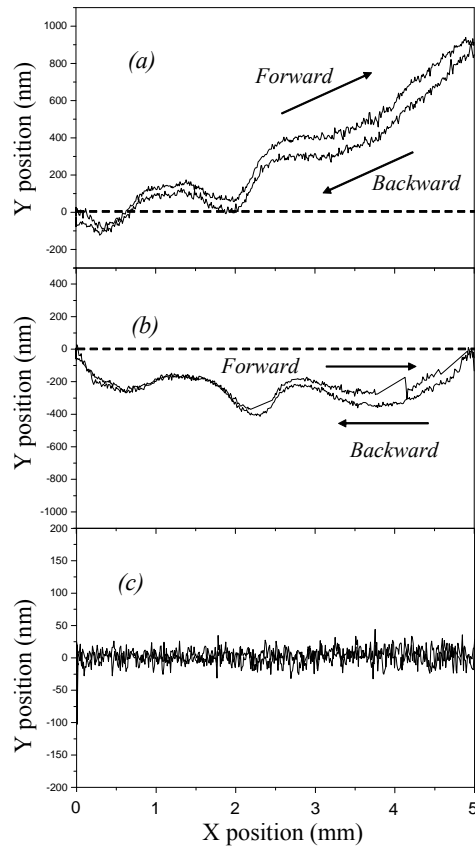
Figure 7: Measurement and tuning of the orthogonality between axes. The dotted line corresponds to the ideal path. The velocity of the displacement is 1 mm.s^{-1} and the data acquisition rate is 1.5 kHz. Part (a) illustrates the displacement before without any tuning sequence. The target point is different to the expected one because of the straightness and orthogonality defects of the ST1 stage. ε_Y is equal to 900 nm which corresponds to an angle of 180 µrad. Part (b) illustrates the same motion after tuning the rotating stage. Although the shift on the target position has been annoyed, the hysteresis and the defects of the stages are still present. In Part (c) these residual effects are compensated using the PSE position control.

Finally, we compensate the residual defect along the Y axis using the PSE position control system as reported in figure 7(c). The data acquisition rate is 1.5 kHz without averaging leading to straightness equal to 9.7 nm. This value can be meaningfully decreased by lowering speed or increasing averaging time. However we demonstrate the dynamic performances of the system and shows that the displacement can be controlled even over millimetre ranges with a high velocity.

4. Conclusion

We have developed a home-made electronic board associated with a heterodyne interferometer which allows us to control the displacement of a XY translation stage at a nanometric level over millimetre range. Some outstanding points of our method have to be noticed. Firstly, it permits to achieve a high level of repeatability. It assures the traceability of the measurement as the nominal frequency laser is one of those recommended by the Comité International des Poids et Mesures to define the Mètre. Furthermore, the nonlinearity of the piezoelectric actuator, the creep and the mechanical defects of the holding sample are not relevant. This work is a part of an integrated project in Nanoscience field.

References

[1] Fahlbusch St, Mazerolle S, Breguet J-M, Steinecker A, Agnus J, Pérez R and Michler J 2005 Nanomanipulation in a scanning electron microscope, *Journal of Materials Processing technology* **167** 371-382

[2] Mizumoto H, Yabuya M, Shimizu T and Kami Y 1995 An angstrom-positioning system using a twist-roller friction drive, *Prec. Eng.* **14** 57-62

[3] Hwang J, Park C-H, Lee C-H and Kim S-W 2005 Estimation and correction method for the two-dimensional position errors of a planar XY stage based on motion error measurements, *International Journal of Machine Tools & manufacture*, 1-12

[4] Gao W, Arai Y, Shibuya A, Kiyono S and Park C-H 2006 Measurement of multi-degree-of-freedom error motions of a precision linear air-bearing stage, *Prec. Eng.* **30** 96-103

[5] The international technology Roadmap for semiconductors, Metrology report 2005 http://www.itrs.net/Common/2005ITRS/Metrology2005.pdf

[6] Lee C-W and Kim S-W 1997 An ultraprecision stage for alignment of wafers in advanced microlithography, *Prec. Eng.* **21** 113-122

[7] Meli F and Thalmann R 1998 Long range AFM profiler used for accurate pitch measurements, *Meas. Sci. Technol.* **9** 1087-1092

[8] Chu C-L and Fan S-H 2006 A novel long-travel piezoelectric-driven linear nanopositioning stage, *Prec. Eng.* **30** 85-95

[9] Liu H, Lu B, Ding Y, Tang Y and Li D 2003 A motor-piezo actuator for nano-scale positioning based on dual servo loop and nonlinearity compensation, *J. Micromech. Microeng.* **13** 295-299

[10] Fu J, Young R D and Vorburger T V 1992 Long range scanning for scanning tunnelling microscopy, *Rev. Sci. Instrum.* **63** 2200-2205

[11] Yeh H-C, Ni W-T and Pan S-S 2005 Digital closed-loop nanopositioning using rectilinear flexure stage and laser interferometry, Control Engineering Practice **13** 559-566

[12] Holmes M, Hocken R and Trumper D 2000 The long-range scanning stage: a novel platform for scanned-probed microscopy, *Prec. Eng.* **24** 191-209

[13] Haycocks J and Jackson K 2005 Traceable calibration of transfer standards for scanning probe microscopy, *Prec. Eng.* **29** 168-175

[14] Leach R, Haycocks J, Jackson K, Lewis A, Oldfield S and Yaccot A 2001 Advances in traceable nanometrology at the National Physical Laboratory, *Nanotechnology* **12** R1-R6

[15] Misumi I, Gonda S, Kurosawa T, Azuma Y, Fujimoto T, Kojima I, Sakurai T, Ohmi T and Takamasu K 2006 Reliability of parameters of associated base straight line in step height samples: Uncertainty evaluation in step height measurements using nanometrological AFM, *Prec. Eng.* **30** 13-22

[16] Topçu S, Chassagne L, Haddad D, Alayli Y and Juncar P 2003 Heterodyne interferometric technique for displacement control at sub-nanometric scale, *Rev. Sci. Instrum.* **74** 4875-4880

[17] Demarest F C 1998 High resolution, high speed, low data age uncertainty, heterodyne displacement measuring interferometer electronics, *Meas. Sci. Technol.* **9** 1024-1030

[18] Chassagne L, Topcu S, Alayli Y and Juncar P 2005 Highly accurate positioning control method for piezoelectric actuators based on phase-shifting optoelectronics, *Meas. Sci. Technol.* **16** 1771-1777

[19] Birch K P and Downs M J 1993 *Metrologia* **30** 155

[20] Sutton C M 1987 Non-linearity in length measurement using heterodyne Michelson interferometry, *Phys. E: Sci. Instrum.* **20** 1290-1292

[21] Wu C and Su C 1996 Non-linearity in measurements of length by optical interferometry, *Meas. Sci. Technol.* **7** 62-68

[22] Rosenbluth A E and Bobroff N 1990 Optical sources of non-linearity in heterodyne interferometers, *Prec. Eng.* **12** 7-11

[23] Topçu S, Chassagne L, Alayli Y and Juncar P 2005 Improving the accuracy of homodyne Michelson interferometers using polarization state measurement techniques, *Opt. Commun.* **247** 133-139

[24] Topçu S, Chassagne L, Haddad D, Alayli Y and Juncar P 2004 High accuracy velocity control method for the French moving coil watt balance, *Rev. Sci. Instrum.* **75** 4824-4827

[25] Bobroff N 1993 Critical alignment in plane mirror interferometry, *Prec Eng.* **15** 33-38